KLF10 upregulates ACSM3 via the PI3K/Akt signaling pathway to inhibit the malignant progression of melanoma

ZHIRONG ZHAO[1], YUANCHANG ZHAN[2], LI JING[3] and HUALI ZHAI[4]

[1]Department of Clinical Laboratory, Xi'an Dian Medical Laboratory Co., Ltd., Xi'an Shaanxi 210016; [2]Department of Clinical Laboratory, Xi'an Aerospace General Hospital, Xi'an, Shaanxi 710000; [3]Department of Clinical Laboratory Jingbian County People's Hospital, Yulin, Shaanxi 718500; [4]Department of Clinical Laboratory, Changan Hospital, Xi'an, Shaanxi 710000, P.R. China

Received September 16, 2021; Accepted January 19, 2022

DOI: 10.3892/ol.2022.13295

Abstract. Malignant melanoma is a type of skin cancer caused by mutations in the DNA of melanocytes. Melanoma is relatively rare compared with other types of skin tumors, but has a highly aggressive biological behavior and consequently, a poorer prognosis. Therefore, the present study aimed to explore the role and mechanism of Kruppel-like factor 10 (KLF10) and acyl-CoA medium-chain synthetase 3 (ACSM3) in melanoma progression. KLF10 expression in melanoma tissues was predicted using Gene Expression Profiling Interactive Analysis (GEPIA). KLF10 expression in healthy and melanoma cells was also detected using reverse transcription-quantitative PCR and western blotting. Cell transfection was performed to overexpress KLF10 or silence ACSM3. Cell viability, proliferation, migration, invasion and apoptosis were detected using Cell Counting Kit-8, colony formation, wound healing, Transwell and TUNEL assays, respectively. The activity of the ACSM3 promoter was detected using a dual-luciferase reporter assay, and the relationship between KLF10 and ACSM3 was detected using the GEPIA database and chromatin immunoprecipitation (ChIP). The results demonstrated that KLF10 expression was significantly downregulated in melanoma cells, especially in A375 cells. Compared with the Ov-NC group, KLF10 overexpression significantly inhibited the proliferation, invasion and migration of melanoma cells and promoted their apoptosis. Similar to KLF10, ACSM3 was also downregulated in A375 cells compared with that in the HEM group, and the GEPIA database analysis and ChIP assay results demonstrated that KLF10 expression was positively associated with ACSM3 expression. Furthermore, silencing ACSM3 significantly reversed the effect of KLF10 overexpression on cell proliferation, invasion and migration, and ACSM3 knockdown increased the levels of phosphorylated (p)-PI3K and p-Akt compared with the levels in the Ov-KLF10 + sh-NC group. Overall, the present study suggested that KLF10 inhibited the proliferation, invasion and migration of melanoma cells by targeting ACSM3 via the PI3K/Akt signaling pathway.

Correspondence to: Dr Huali Zhai, Department of Clinical Laboratory, Changan Hospital, 9 Fengcheng Third Road, Weiyang, Xi'an, Shaanxi 710000, P.R. China
E-mail: huali1012021@163.com

Key words: malignant melanoma, Kruppel-like factor 10, acyl-CoA medium-chain synthetase 3, PI3K/AKT signaling pathway, invasion, migration, apoptosis

Introduction

Melanoma is one of the most malignant skin tumors worldwide and the incidence of melanoma continues to increase, with an age standardized incidence rate of 3.1 per 100,000/year, particularly in Caucasian populations (1). The average age of onset of melanoma is ~50 years (2). Although melanoma is a rare disease, it has a high mortality rate of 1.7 per 100,000/year in Europe (1). As melanocytes are located in the basal layer of the epidermis, melanoma is most common on the skin, accounting for 75% of all skin cancer-associated deaths (3). In 2019, 96,480 new cases of melanoma were estimated to have been diagnosed, with a total of 7,230 deaths as a result of melanoma in the United States alone (4). The clinically distinguishable subtypes of melanoma are as follows: Cutaneous, mucosal, uveal and unknown primary melanoma (5). At present, melanoma is mainly treated via surgery, supplemented with radiotherapy and chemotherapy (6). However, due to the toxicity and side effects of radiotherapy and chemotherapy, novel therapeutic approaches need to be identified. Therefore, the present study aimed to identify novel therapeutic targets and novel therapeutic strategies for the treatment of melanoma. However, the molecular mechanisms that serve a role in melanoma remain to be elucidated.

Kruppel-like factor 10 (KLF10), formerly known as TGF-β induction early gene 1, is a DNA-binding transcriptional regulator that contains a triple C2H2 zinc finger domain (7). In numerous types of cancer, KLF10 upregulation reduces cancer cell proliferation. For example, a previous study demonstrated that KLF10 expression is negatively associated with progression-free and overall survival of patients with pancreatic cancer and could be used as a predictor of pancreatic cancer stage (8). Under the regulation of microRNA-106b-5p, KLF10 inhibits the proliferation of several types of myeloma cells

via the regulation of pituitary tumor-transforming gene 1 (9). Jin *et al* (10) reported that KLF10 inhibits the proliferation and invasion of breast cancer cells by inhibiting the transcription of EGFR. Therefore, it can be hypothesized that KLF10 serves an important role in inhibiting cancer cell proliferation and promoting apoptosis, which strongly suggests that it may be a tumor suppressor. However, limited information is available regarding its mechanism of action in melanoma cells.

Similar to KLF10, acyl-CoA medium-chain synthetase 3 (ACSM3) serves a role in several types of cancer. Previous studies have used the Gene Expression Omnibus (https://www.ncbi.nlm.nih.gov/gds), The Cancer Genome Atlas (http://www.cbioportal.org/) and Human Protein Atlas (https://www.proteinatlas.org/) databases to determine the differential expression of ACSM3. It has previously been demonstrated that ACSM3 expression is downregulated in malignant melanoma and that low ACSM3 expression is associated with a poor prognosis of melanoma (11). Furthermore, upregulation of ACSM3 inhibits integrin β1/Akt signaling, which inhibits the progression of ovarian cancer (12). Additionally, upregulation of ACSM3 reduces the migration and invasion of liver cancer cells *in vivo* and *in vitro*, and downregulates the phosphorylation of lysine-deficient protein kinase 1 and Akt (13).

It was hypothesized that KLF10 might inhibit melanoma progression by targeting ACSM3. Previous bioinformatics analyses have demonstrated that the expression levels of KLF10 and ACSM3 are decreased in melanoma cell lines (11,14). However, to the best of our knowledge, the effects of KLF10 and ACSM3 in melanoma on the proliferation, invasion, migration and apoptosis of tumor cells, remain unclear. Therefore, the present study investigated the effects of KLF10 and ACSM3 on the proliferation, invasion, migration and apoptosis of tumor cells, and their mechanisms, in order to find novel therapeutic targets for melanoma.

Materials and methods

Cell culture and treatment. The human normal epidermal melanocyte (HEM; cat. no. PCS-200-012) cell line and melanoma cell lines (SK-MEL-1, cat. no. HTB-67; A2058, cat. no. CRL-11147; RPMI-7951, cat. no. HTB-66; and A375, cat. no. CRL-1619) were obtained from the American Type Culture Collection. All cell lines were cultured in DMEM (HyClone; Cytiva) supplemented with 10% FBS (HyClone; Cytiva) and 1% antibiotics (100 U/ml penicillin and 100 mg/ml streptomycin; Gibco; Thermo Fisher Scientific, Inc.) at 37˚C with 5% CO_2.

Bioinformatics analysis. The expression levels of KLF10 and ACSM3 and their correlation in the tissues of patients with cutaneous melanoma, as well as the relationship between low ACSM3 expression and overall and disease-free survival in cutaneous melanoma patients were predicted using Gene Expression Profiling Interactive Analysis (GEPIA; http://gepia.cancer-pku.cn/). The JASPAR database (http://jaspar.genereg.net/) was used to predict the binding site of transcription factor KLF10 to the ACSM3 promoter.

Cell transfection. A375 cells ($3x10^5$ cells/well) were inoculated onto 6-well plates and cultured for 24 h at 37˚C with 5% CO_2. Following incubation, cells were transfected with the pCDNA3.1 vector targeting KLF10 (Ov-KLF10), the negative control (NC) empty vector (Ov-NC), the pGPH1 vector carrying short hairpin RNA-ACSM3 (sh-ACSM3; 5'-GGTTTAGGATTATCTGTAA-3') and its negative control (sh-NC; 5'-TTCGGGTCATCCGATGGGCC-3') at a concentration of 25 nM. All plasmids were synthesized by Shanghai GenePharma Co., Ltd. and transfected using Lipofectamine® 2000 (Invitrogen; Thermo Fisher Scientific, Inc.) according to the manufacturer's protocol. Blank control group cells were untransfected. Following transfection for 48 h at 37˚C, the transfection efficiency was detected using reverse transcription-quantitative PCR (RT-qPCR) and western blotting.

Cell Counting Kit-8 (CCK-8) assay. The CCK-8 assay was performed to assess cell proliferation. Briefly, A375 cells were seeded into a 96-well plate ($5x10^3$ cells/well), and incubated for 24, 48 and 72 h at 37˚C with 5% CO_2. Following incubation, 10 μl CCK-8 solution (cat. no. P0037; Beyotime Institute of Biotechnology) was added into each well and the cells were cultured for another 2 h at 37˚C with 5% CO_2. The optical density at 450 nm was detected using a microplate reader (BioTek Instruments, Inc.).

Colony formation assay. Transfected A375 cells ($3x10^2$ cells/well) were digested with 0.25% trypsin to form a cell suspension, and then cultured in DMEM and inoculated into 6-well plates, with incubation at 37˚C in 5% CO_2 for 14 days. The cells were fixed with 70% ethanol at room temperature (20-25˚C) for 15 min and stained with 0.05% crystal violet at 37˚C for 20 min. The number of colonies formed was counted (≥50 cells/colony) manually using an Olympus BX40 light microscope (Olympus Corporation).

TUNEL assay. Apoptosis was detected using One Step TUNEL Apoptosis Assay Kit (Beyotime Institute of Biotechnology) according to the manufacturer's protocol at 37˚C for 60 min. Briefly, the A375 cells were washed with PBS three times and then fixed at room temperature (20-25˚C) with 4% paraformaldehyde (Beyotime Institute of Biotechnology) for 15 min. Subsequently, 0.15% Triton-X-100 was added to the cells at room temperature for a further 5 min. Terminal deoxynucleotidyl transferase solution and FITC-deoxyuridine triphosphate solution (Roche Diagnostics GmbH) were added to the cells and the cells were incubated at 37˚C for 60 min in the dark. DAPI (0.5 μg/ml) was adopted to stain the nuclei for 5 min at room temperature. The detection solution was discarded and cells were washed three times with PBS. Antifade Mounting Medium was used to seal the cells. Cells were randomly selected from 5 fields of view and an inverted fluorescence microscope (Olympus Corporation) was used to observe excitation and emission wavelengths within the range of 450-500 and 515-565 nm (green fluorescence), respectively. Apoptosis index=number of apoptotic cells/(number of apoptotic cells + normal cells).

Wound healing assay. A375 cells were inoculated in 6-well plates ($1x10^5$ cells/well). When the cells reached 70-80% confluence, the medium was replaced with serum-free DMEM and the cells were incubated overnight at 37˚C with

5% CO_2. Subsequently, a 200-μl sterile pipette tip was used to scratch the cell monolayer. After washing with PBS three times, the plates were maintained at 37˚C with 5% CO_2. Images were captured at 0 and 24 h using a BX51 inverted light microscope (magnification, x100; Olympus Corporation). The area of wound closure in each picture was determined by using ImageJ software (version. 1.52; National Institutes of Health). The percentage of migration was calculated as follows: % migration=scratch current width/scratch original width x100.

Cell invasion assay. Cell invasion was assessed using Transwell chambers coated with Matrigel (BD Biosciences). The 24-well Transwell plates (Corning, Inc.) with 8-μm pore inserts were coated with Matrigel (BD Biosciences) at 37˚C for 30 min. Subsequently, $4x10^4$ A375 cells were placed in serum-free medium. The upper chamber was precoated with matrix (Sigma-Aldrich; Merck KGaA) and the cells were added to the upper chamber (0.1 ml cell suspension/well), whereas the lower chamber was filled with cell culture medium supplemented with 20% FBS. Following incubation at 37˚C with 5% CO_2 for 24 h, the invading cells were fixed with 4% formaldehyde at 25˚C for 15 min and stained with 0.3% crystal violet solution (Sigma-Aldrich; Merck KGaA) at room temperature for 30 min. The invading cells were observed under an inverted light microscope (magnification, x100; Olympus Corporation) in five randomly selected fields of view. Percentage invasion was calculated as follows: % invasion=invaded cells in lower chamber/total cells added to top chamber x100.

RT-qPCR. Total RNA was extracted from cells using RNAzol® RT (Sigma-Aldrich; Merck KGaA) according to the manufacturer's protocol. Subsequently, RNA was reverse transcribed into complementary DNA (cDNA) using a QuantiTect Reverse Transcription Kit (Qiagen GmbH) at 42˚C for 1 h. The obtained cDNA was amplified via qPCR using SYBR Select MasterMix (Takara Bio, Inc.) on the ABI7500 Sequence Detection System (Applied Biosystems) according to the detection system manufacturer's protocol. The thermocycling conditions were 50˚C for 2 min, followed by 95˚C for 15 sec, 60˚C for 15 sec and 72˚C for 1 min for a total of 40 cycles. The $2^{-\Delta\Delta Cq}$ method (15) was used to quantify relative mRNA expression levels using GAPDH as the internal reference gene. The sequences of the qPCR primers were as follows: KLF10 forward, 5'-ACCCAG GGTGTGGCAAGAC-3' and reverse, 5'-AGCGAGCAAACC TCCTTTCA-3'; ACSM3 forward, 5'-AGGAAGATGCTACGT CATGCC-3' and reverse, 5'-ATCCCCAGTTTGAAGTCC TGT-3'; and GAPDH forward, 5'-ACCACAGTCCATGCC ATCAC-3' and reverse, 5'-TCCACCACCCTGTTGCTGTA-3'.

Western blotting. A375 cells were washed three times with pre-cooled PBS, and total protein was extracted from the cells using RIPA lysis buffer (Beyotime Institute of Biotechnology). The total protein concentration was determined using a Pierce BCA Protein Assay Kit (Thermo Fisher Scientific, Inc.). Following denaturation in a 95˚C metal bath, SDS-PAGE was performed with a 12% gel for 30-μg protein samples. Separated protein was transferred to PVDF membranes (Beyotime Institute of Biotechnology), which were blocked with 5% skimmed milk for 1 h at room temperature. Subsequently, the membranes were incubated overnight at 4˚C with the following primary antibodies (all purchased from Abcam): KLF10 (dilution, 1:1,000; cat. no. ab184182), Bcl-2 (dilution, 1:1,000; cat. no. ab194583), Bax (dilution, 1:1,000; cat. no. ab32503), caspase 3 (dilution, 1:5,000; cat. no. ab32351), cleaved-caspase 3 (dilution, 1:1,000; cat. no. ab32042), MMP2 (dilution, 1:1,000; cat. no. ab92536), MMP9 (dilution, 1:1,000; cat. no. ab76003), ACSM3 (dilution, 1:1,000; cat. no. ab238682), phosphorylated (p)-PI3K (dilution, 1:500; cat. no. ab154598), p-Akt (dilution, 1:1,000; cat. no. ab38449), PI3K (dilution, 1:1,000; cat. no. ab191606), Akt (dilution, 1:1,000; cat. no. ab8805) and GAPDH (dilution, 1:1,000; cat. no. ab181602). After washing twice with PBS, membranes were treated with goat anti-rabbit HRP-binding IgG secondary antibody (dilution, 1:5,000; cat. no. ab6721; Abcam) at room temperature for 1 h. Protein bands were detected using ECL reagent (MilliporeSigma). Bands were semi-quantified and normalized using ImageJ v1.46 software (National Institutes of Health).

Chromatin immunoprecipitation (ChIP)-PCR assay. According to the manufacturer's protocol, total genomic DNA was isolated using the EZChip™ Kit (MilliporeSigma). A total of $2x10^6$ A375 cells were transfected with pCDNA3.1 or pGPH1 vectors and lysed with 250 μl SDS Lysis Buffer (Beyotime Institute of Biotechnology). Next, the A375 cells were sonicated on ice and fragments of DNA were then resolved using a 2% agarose gel. For ChIP, samples were diluted in a 10X ChIP dilution buffer and pre-cleared with 60 μl protein G-agarose beads mixed at 4˚C for 1 h. During chromatin separation, the chromatin was centrifuged at 15,000 x g at 4˚C for 10 min to remove the insoluble matter and then pre-cleared chromatin was incubated with 1 μl antibodies against KLF10 (dilution, 1:100; cat. no. sc-130408; Santa Cruz Biotechnology, Inc.) at 4˚C overnight. The precipitates were washed with low-salt wash buffer, high-salt wash buffer and LiCI wash buffer, and rinsed with TE buffer twice. Immunochromatin was centrifuged at 15,000 x g for 10 min at 4˚C and boiled, and then was amplified via PCR as aforementioned.

Dual-luciferase reporter assay. A375 cells were inoculated in a 24-well plate ($1x10^5$ cells/well). When cells reached 80% confluency, luciferase activity was detected using the Promega Double Fluorescence Detection Kit (Promega Corporation) according to the manufacturer's protocol. ACSM3-wild-type (WT) and ACSM3 mutant reporter plasmids were constructed in advance through the PGL3-CMV-LUC-MCS provided by Genomeditech, A375 cells were transiently co-transfected with Ov-KLF10 together with 0.1 μg ACSM3-WT and ACSM3 mutant reporter plasmids using Lipofectamine 2000 (Invitrogen; Thermo Fisher Scientific, Inc.) for 24 h. Subsequently, 120 μl cell lysate was added to each well and was shaken on a horizontal oscillator for 45 min at 50 x g. Then, 10 μl lysed cell mixture and 50 μl firefly luciferase reagent were added to a 1.5-ml tube and mixed. Prior to assessment, 50 μl Stop/Glo Sealing Luciferase Reagent was added. Firefly luciferase/*Renilla* luciferase values were recorded and the ACSM3 promoter transfer activity was analyzed. Each group was set up with three wells and each experiment was repeated three times.

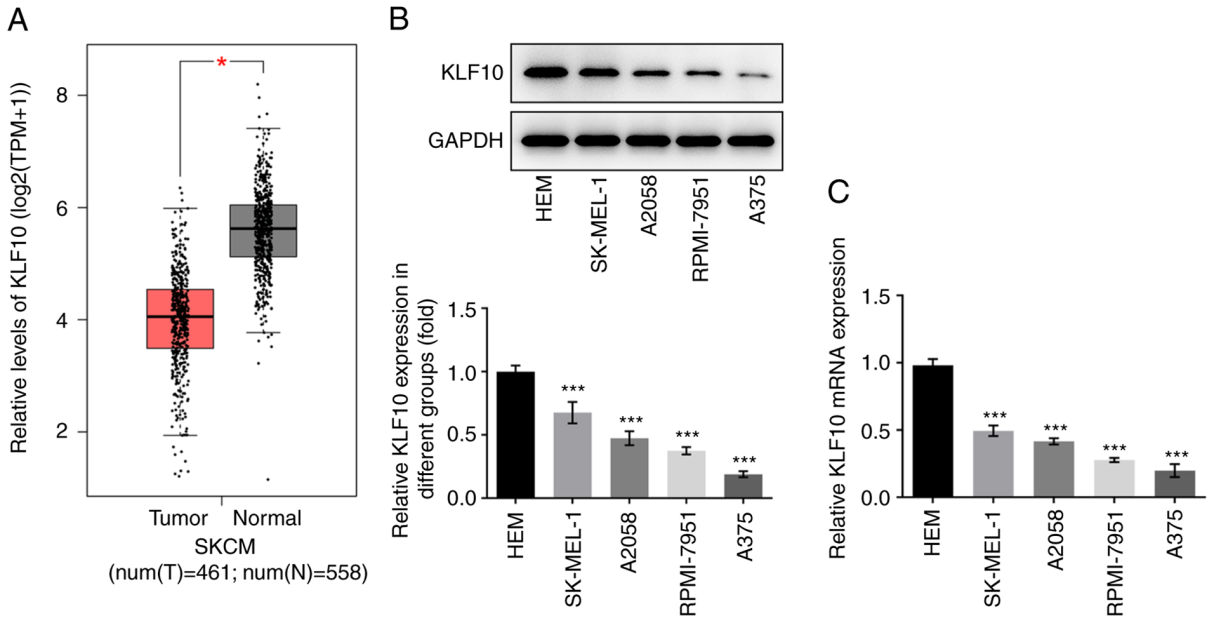

Figure 1. KLF10 is downregulated in melanoma cells. (A) The Gene Expression Profiling Interactive Analysis website was used to investigate KLF10 expression in the tissues of patients with melanoma. (B) Western blotting and (C) reverse transcription-quantitative PCR were used to detect the expression levels of KLF10 in melanoma cells. *P<0.05, ***P<0.001 vs. HEM. KLF10, Kruppel-like factor 10; N, normal; SKCM, skin cutaneous melanoma; T, tumor.

Statistical analysis. Data are presented as the mean ± SD of three or more independent experiments. GraphPad Prism 8.0.2 software (GraphPad Software, Inc.) was used for data analysis. Statistical differences were determined using one-way ANOVA followed by Tukey's post hoc test for group comparisons. The correlation between ACSM3 and KLF10 was evaluated using Pearson's correlation analysis. P<0.05 was considered to indicate a statistically significant difference.

Results

KLF10 expression is relatively low in melanoma tissues and cell lines. KLF10 expression levels in melanoma were examined using GEPIA. Compared with that in healthy tissues, KLF10 expression was significantly decreased in melanoma tissues (Fig. 1A). Western blotting (Fig. 1B) and RT-qPCR (Fig. 1C) were also used to detect KLF10 expression in melanoma cell lines. Compared with that of other melanoma cell lines, including HEM, SK-MEL-1, A2058 and RPMI-7951, KLF10 expression was lowest in A375 cells. Therefore, A375 cells were selected for the subsequent experiments.

KLF10 overexpression inhibits melanoma cell proliferation and induces apoptosis. To investigate the specific role of KLF10 in A375 cells, cells overexpressing KLF10 were analyzed using western blotting (Fig. 2A) and RT-qPCR (Fig. 2B). Compared with that in the Ov-NC group, KLF10 expression was significantly increased in the Ov-KLF10 group. Following KLF10 overexpression, CCK-8 (Fig. 2C) and colony formation (Fig. 2D) assays were used to detect cell proliferation. The results demonstrated that KLF10 overexpression significantly inhibited A375 cell proliferation compared with the Ov-NC group. Furthermore, apoptosis was detected using a TUNEL assay. The results demonstrated that the green fluorescence in the Ov-KLF10 group was significantly enhanced compared with the Ov-NC group (Fig. 2E), which indicated that significant apoptosis had occurred in the cells with overexpression. Subsequently, the expression levels of apoptosis-related proteins were detected via western blotting (Fig. 2F). Compared with those in the Ov-NC group, the expression levels of the antiapoptotic protein Bcl-2 were significantly decreased, whereas the expression level of the proapoptotic proteins Bax and cleaved caspase-3/caspase 3 ratio were significantly increased, in the Ov-KLF10 group. The results suggested that overexpression of KLF10 may promote melanoma cell apoptosis.

KLF10 overexpression inhibits melanoma cell invasion and migration. Transwell and wound-healing assays were used to detect cell invasion and migration. Compared with that in the Ov-NC group, cell migration (Fig. 3A) and invasion (Fig. 3B) were significantly decreased in the Ov-KLF10 group. Additionally, KLF10 overexpression inhibited the expression of metastasis-related proteins MMP2 and MMP9 in A375 cells (Fig. 3C). These results indicated that KLF10 may inhibit A375 cell invasion and migration.

KLF10 promotes the transcription of ACSM3. Results obtained using GEPIA indicated that ACSM3 expression was low in melanoma tissues (Fig. 4A). Furthermore, the overall survival rate and disease-free survival rate of patients with melanoma were positively associated with high ACSM3 expression (Fig. 4B and C). Bioinformatics analysis also demonstrated that the expression levels of KLF10 and ACSM3 were positively associated in patients with melanoma (Fig. 4D). Subsequently, western blotting (Fig. 4E) and RT-qPCR (Fig. 4F) were performed to detect ACSM3 expression in HEM and A375 cell lines. Compared with that in HEM cells, ACSM3 mRNA and protein expression was downregulated in A375 cells. Furthermore, the binding sites between KLF10 and

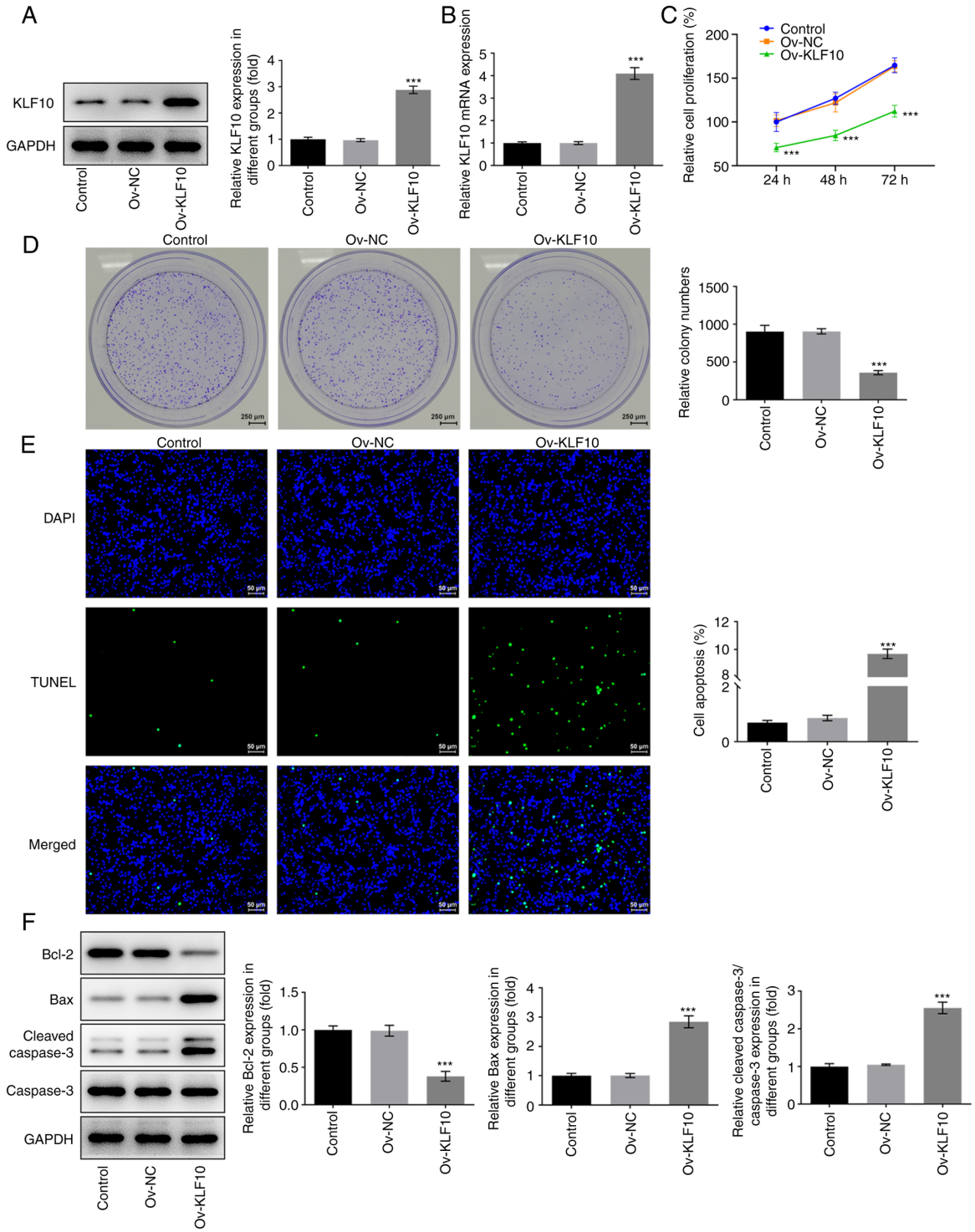

Figure 2. Overexpression of KLF10 inhibits proliferation and induces apoptosis of melanoma cells. (A) Western blotting and (B) reverse transcription-quantitative PCR were used to detected the expression levels of KLF10. (C) A Cell Counting Kit-8 assay was used to detect the levels of cell proliferation. (D) A colony formation assay was used to detect the cell cloning levels. Scale bar, 250 μm. (E) Cell apoptosis was detected by TUNEL staining. Scale bar, 50 μm. (F) Expression levels of apoptosis-related proteins (Bax, Bcl-2 and cleaved caspase 3) were examined by western blotting. ***P<0.001 vs. Ov-NC. KLF10, Kruppel-like factor 10; NC, negative control; Ov, overexpression.

ACSM3 were predicted using the JASPAR database (Fig. 4G). In the presence of the wild-type ACSM3 promoter, KLF10 overexpression induced a significant increase in luciferase activity, whereas there was no significant change in the presence of the mutant promoter (Fig. 4H). These results suggested that KLF10 directly upregulated ACSM3 by binding to the ACSM3 promoter. Considering the positive association between KLF10 and ACSM3 expression, a ChIP assay was performed to further verify the binding of KLF10 and ACSM3. It was found that co-transfected ACSM3 wild-type and Ov-KLF10 A375 cells showed more relative luciferase activity (Fig. 4H). ACSM3 was present in the KLF10 fraction, which revealed that ACSM3 may bind to KLF10 (Fig. 4I). Furthermore, it was demonstrated that ACSM3 mRNA and protein expression was

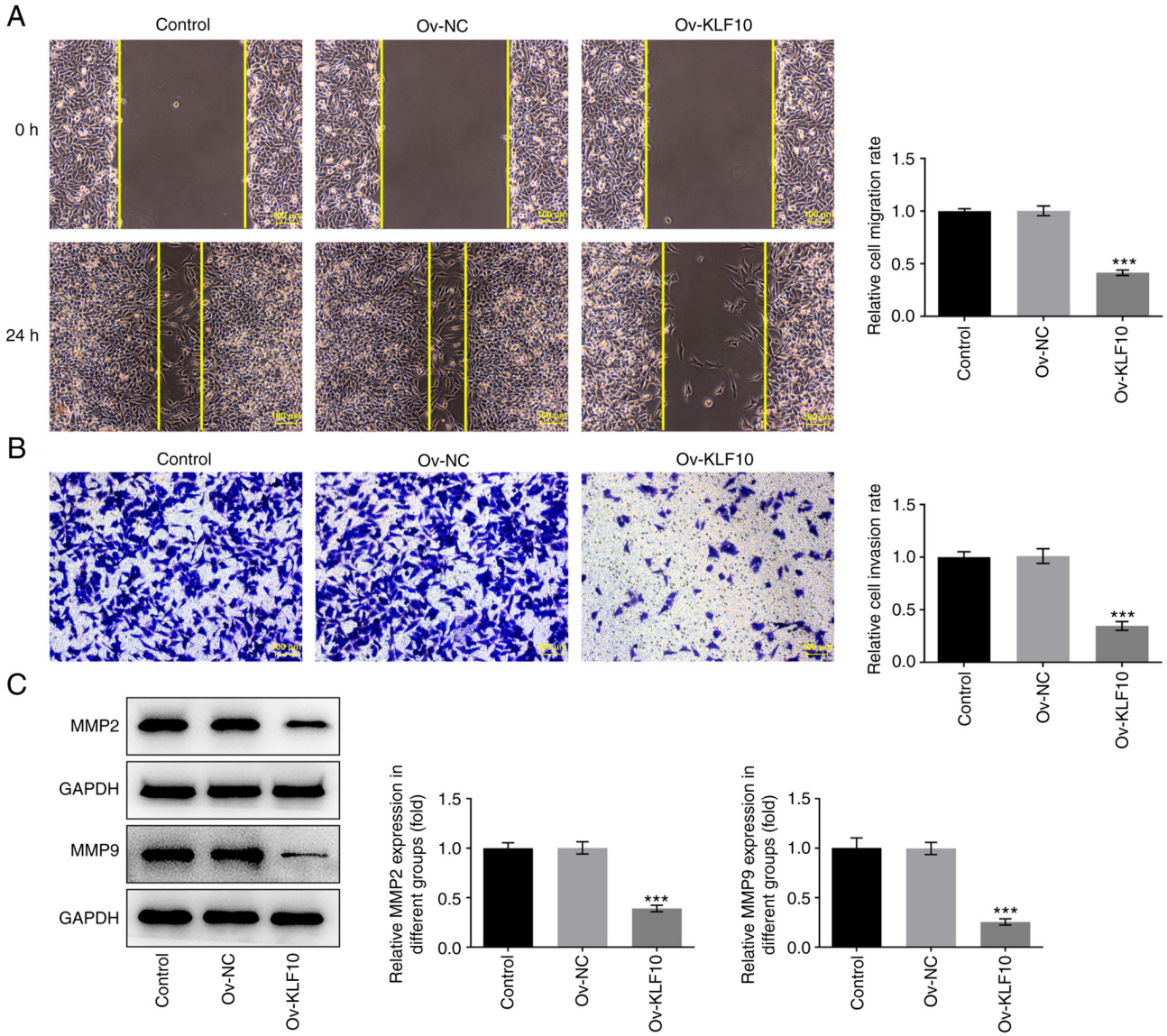

Figure 3. Overexpression of KLF10 inhibits the invasion and migration of melanoma cells. (A) Wound-healing and (B) Transwell assays were used to detect the levels of migration and invasion of melanoma cells. Scale bar, 100 μm. (C) Expression levels of metastasis-related proteins (MMP2 and MMP9) were detected by western blotting. ***P<0.001 vs. Ov-NC. KLF10, Kruppel-like factor 10; NC, negative control; Ov, overexpression.

upregulated in A375 cells overexpressing KLF10 compared with in the Ov-NC group (Fig. 4J and K).

KLF10 upregulates ACSM3 and inhibits the malignant progression of melanoma via the PI3K/Akt signaling pathway. To elucidate the mechanism of the inhibition of malignant melanoma progression via the binding of KLF10 to ACSM3, sh-ACSM3 was constructed and transfected into A375 cells. The transfection efficiency was analyzed using western blotting and RT-qPCR. The results demonstrated that ACSM3 mRNA and protein expression in the sh-ACSM3 group was significantly decreased compared with that in the sh-NC group (Fig. 5A and B). CCK-8 and colony formation assays were performed to assess cell proliferation. The results demonstrated that cell proliferation was inhibited by KLF10 overexpression compared with that in the control group, which was reversed by sh-ACSM3 as compared with that in the Ov-KLF10 + sh-NC group (Fig. 5C and D).

Furthermore, apoptosis and apoptosis-related proteins were analyzed using the TUNEL assay and western blotting, respectively. Overexpression of KLF10 significantly induced the apoptosis of A375 cells compared with that in the control group, whereas sh-ACSM3 decreased apoptosis in A375 cells transfected with Ov-KLF10 in comparison with that in the Ov-KLF10 + sh-NC group (Fig. 5E). The results of western blotting demonstrated that Bcl-2 protein expression was upregulated and the expression levels of proapoptotic proteins Bax and the cleaved caspase 3/caspase 3 ratio were downregulated in the Ov-KLF10+sh-ACSM3 group compared with those in the Ov-KLF10 + sh-NC group (Fig. 6A). Transwell and wound healing assays were used to detect cell invasion and migration. The results demonstrated that KLF10 overexpression inhibited the invasion and migration of A375 cells, whereas silencing ACSM3 expression enhanced cell invasion and migration (Fig. 6B). Furthermore, KLF10 overexpression inhibited the expression of metastasis-related proteins MMP2

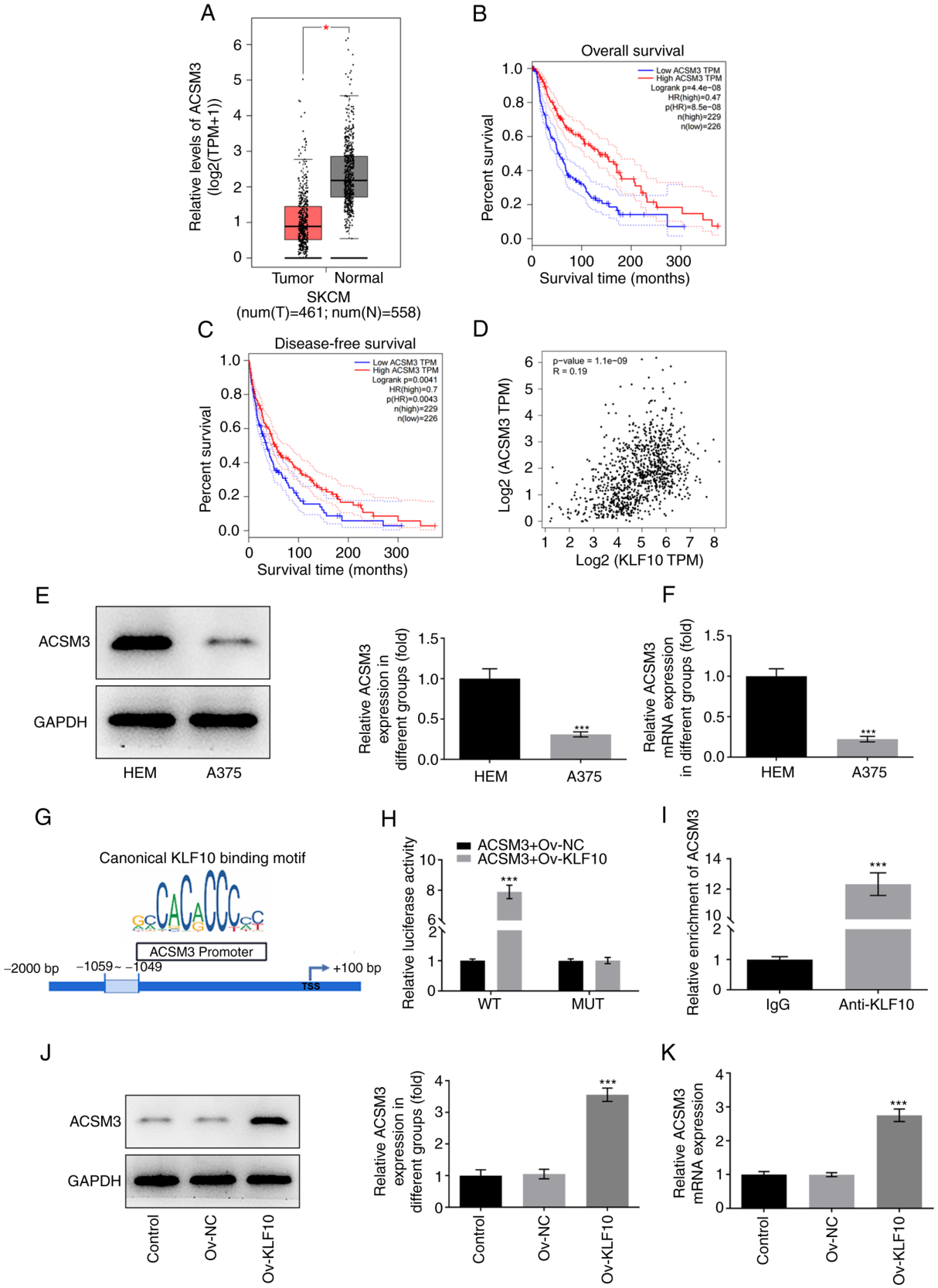

Figure 4. KLF10 binds to ACSM3 and promotes the transcription of ACSM3. (A) The Gene Expression Profiling Interactive Analysis website revealed the expression levels of ACSM3. (B) The association between ACSM3 expression and overall survival rate in melanoma patients, (C) the association of ACSM3 and disease-free survival rate in patients with melanoma, and (D) the association between KLF10 expression and ACSM3 expression in patients with melanoma were examined. (E) Western blotting and (F) RT-qPCR were used to detect the expression levels of ACSM3 in melanoma cells. (G) JASPAR predicted the binding sites of KLF10 and the ACSM3 promoter. (H) Luciferase reporter gene assay was used to detect the ACSM3 promoter activity. (I) Immunoprecipitation further indicated that KLF10 could bind with ACSM3. (J) Western blotting and (K) RT-qPCR were used to detect the expression levels of ACSM3 after KLF10 overexpression. *P<0.05, ***P<0.001 vs. HEM, ACSM3 + Ov-NC, IgG or Ov-NC. ACSM3, acyl-CoA medium-chain synthetase 3; KLF10, Kruppel-like factor 10; MUT, mutant; N, normal; NC, negative control; Ov, overexpression; RT-qPCR, reverse transcription-quantitative PCR; SKCM, skin cutaneous melanoma; T, tumor; TPM, transcripts per million; WT, wild-type.

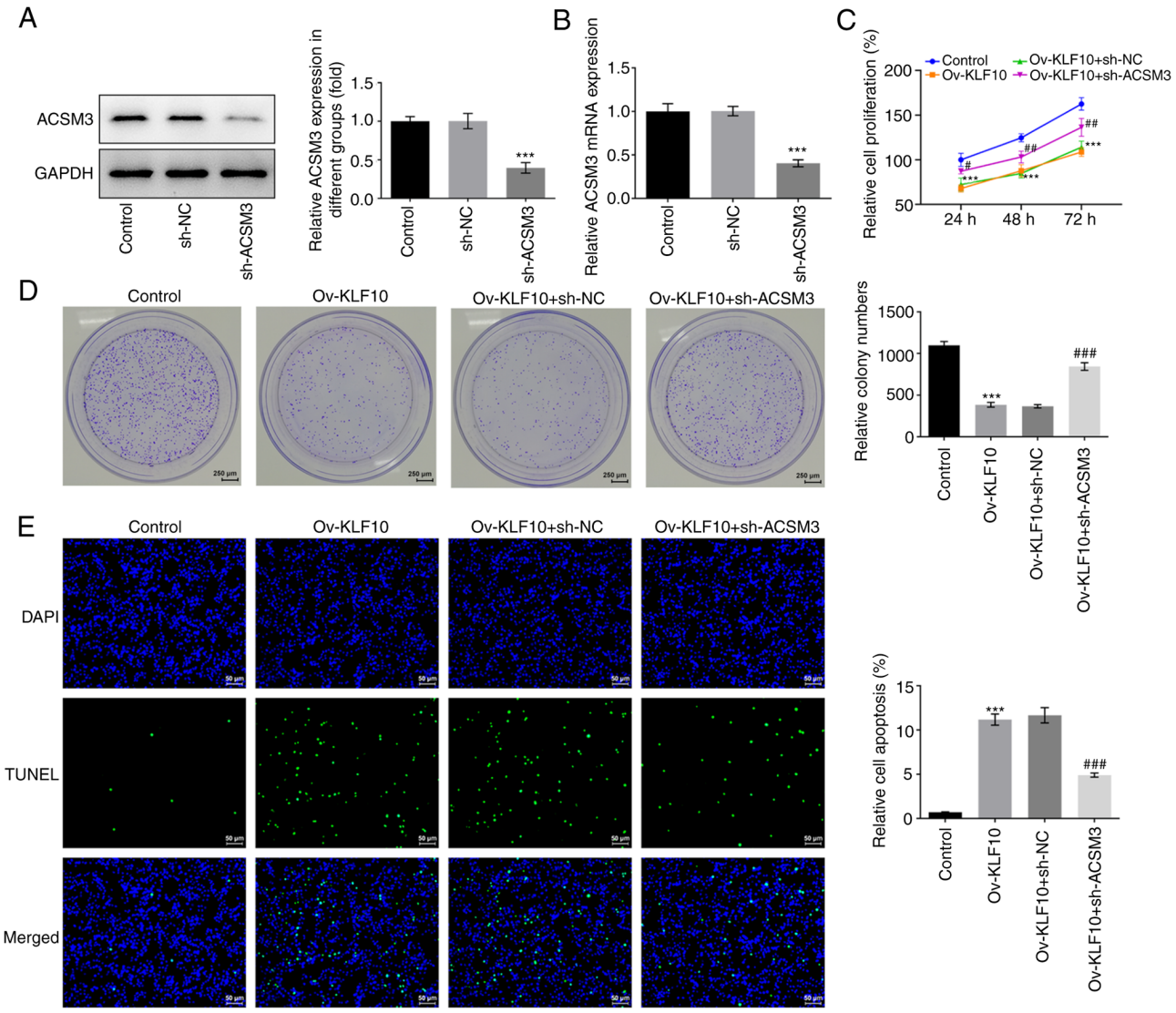

Figure 5. Silencing of ACSM3 reverses the inhibitory effect of KLF10 on melanoma cell viability and proliferation. Detection of ACSM3 silencing by (A) western blotting and (B) reverse transcription-quantitative PCR. (C) A Cell Counting Kit-8 assay was used to detect the levels of cell proliferation. (D) A colony formation assay was used to detect the cell colony levels. Scale bar, 250 μm. (E) Cell apoptosis was detected by TUNEL staining. Scale bar, 50 μm. ***P<0.001 vs. Control; $^{\#}$P<0.05, $^{\#\#}$P<0.01, $^{\#\#\#}$P<0.001 vs. Ov-KLF10 + sh-NC. ACSM3, acyl-CoA medium-chain synthetase 3; KLF10, Kruppel-like factor 10; NC, negative control; Ov, overexpression; sh, short hairpin RNA.

and MMP9 in A375 cells, whereas sh-ACSM3 increased MMP2 and MMP9 expression (Fig. 6C). It has previously been reported that ACSM3 can negatively regulate the Akt signaling pathway (10). Therefore, western blotting was performed to detect the protein expression levels of PI3K/Akt signaling pathway proteins. Compared with the control group, the overexpression of KLF10 significantly reduced the levels of p-PI3K and p-Akt, which was reversed by sh-ACSM3, in contrast to the Ov-KLF10 + sh-NC group (Fig. 7). Overall, these results indicated that KLF10 may upregulate ACSM3 and inhibit the malignant progression of A375 cells via the PI3K/Akt signaling pathway.

Discussion

Melanoma is considered to be the deadliest skin cancer (16-18). In its early stages, melanoma can be successfully treated by surgery alone, and it has a high 5-year survival rate of 92%; however, the 1-year survival rate markedly decreases to 55% following metastasis (19). Understanding the mechanisms that lead to the occurrence of melanoma will provide novel strategies for the diagnosis and treatment of this disease (20). In the present study, KLF10 and ACSM3 expression levels were significantly downregulated in melanoma cell lines, and ACSM3 was closely associated with low overall and disease-free survival in patients with cutaneous melanoma. ACSM3 expression levels were associated with KLF10. Furthermore, KLF10 overexpression significantly inhibited the proliferation, migration and invasion of A375 cells, and induced apoptosis, which were reversed by knockdown of ACSM3.

The KLF10 transcription factor was originally cloned from human osteoblasts and acts as a major response gene in TGF-β therapy (21). Increasing evidence suggests that KLF10 serves an important role in mimicking TGF-β function in a number of types of cancer. For example, Baroy *et al* (22) reported that LSAMP reduces osteosarcoma cell proliferation

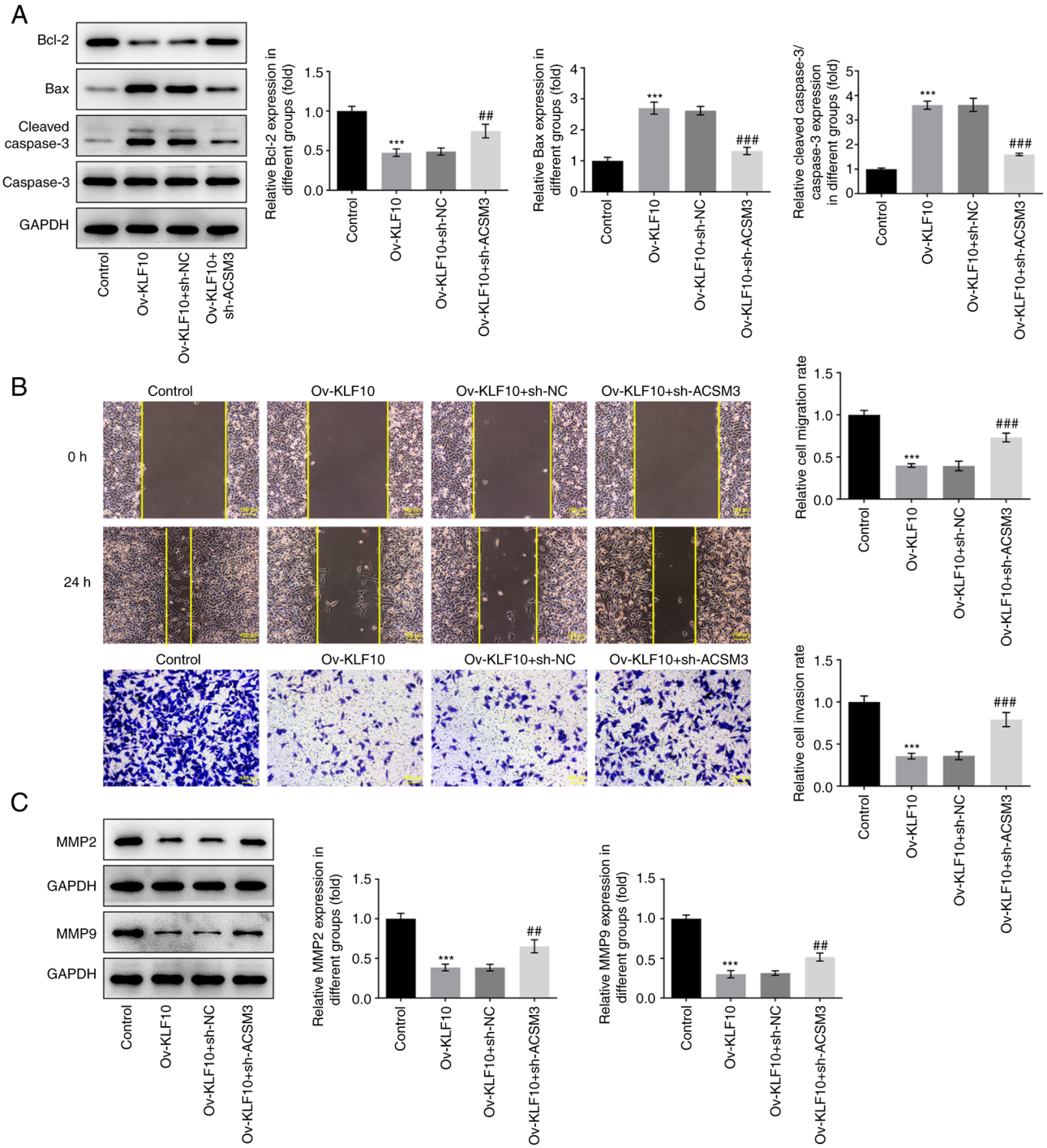

Figure 6. Silencing of ACSM3 reverses the inhibitory effect of KLF10 on melanoma cell apoptosis, migration and invasion. (A) Expression levels of apoptosis-related proteins (Bax, Bcl-2 and cleaved caspase 3) were examined by western blotting. (B) Wound healing and Transwell assays were used to detect cell migration and invasion. Scale bar, 100 μm. (C) Western blotting was used to detect the expression levels of metastasis-related proteins MMP2 and MMP9. ***P<0.001 vs. Control; $^{\#\#}$P<0.01 and $^{\#\#\#}$P<0.001 vs. Ov-KLF10 + sh-NC. ACSM3, acyl-CoA medium-chain synthetase 3; KLF10, Kruppel-like factor 10; NC, negative control; Ov, overexpression; sh, short hairpin RNA.

by indirectly upregulating one or more genes (HES1, CTAG2 or KLF10). Jin *et al* (21) reported that KLF10 is upregulated in apoptosis induced by tetrotylenine or vancomycin, and that overexpression of KLF10 induces apoptosis of K562 cells. Furthermore, Hsu *et al* (23) demonstrated that KLF10 regulation of Bax inhibitor-1 expression and Ca^{2+} release may be a pathway of estrogen-induced apoptosis. This evidence supports the role of KLF10 as a suppressor in several types of cancer; however, to the best of our knowledge, the role of KLF10 in melanoma has not previously been reported. In the present study, the inhibitory effect of KLF10 on the proliferation and survival of A375 cells and its mechanism were investigated. The results determined that KLF10 may also act as a tumor suppressor in melanoma.

ACSM3 has previously been reported to be involved in numerous biological processes, including tumor

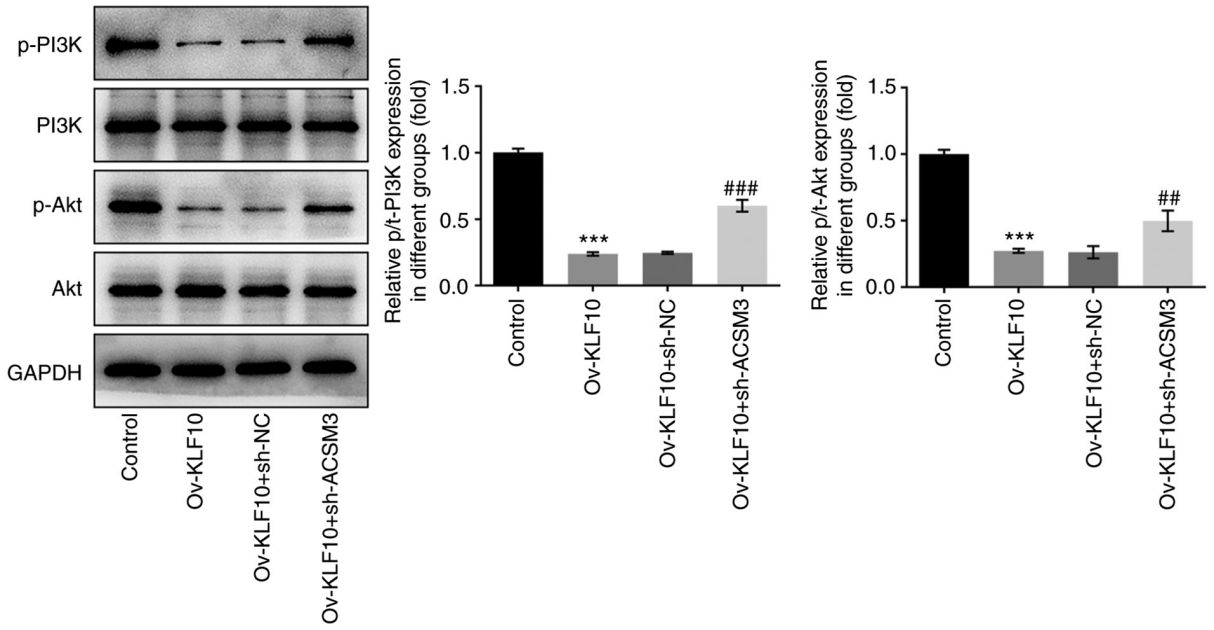

Figure 7. KLF10 upregulates ACSM3 to inhibit the malignant progression of melanoma via the PI3K/Akt signaling pathway. The levels of p-Akt, Akt, P13K and p-P13K in A375 cells were detected by western blotting. ***P<0.001 vs. Control; ##P<0.01 and ###P<0.001 vs. Ov-KLF10 + sh-NC. ACSM3, acyl-CoA medium-chain synthetase 3; KLF10, Kruppel-like factor 10; NC, negative control; Ov, overexpression; p-, phosphorylated; sh, short hairpin RNA.

migration, invasion, fat accumulation and the butyrate oxidation pathway (13,24,25), and particularly in cancer. Gopal *et al* (26) demonstrated that ACSM3 gene expression is decreased in hepatocellular carcinoma (HCC) tissues, whereby the loss of ACSM3 expression is associated with advanced HCC stage and a low survival rate. Zhu *et al* (11) demonstrated that ACSM3 is downregulated in melanoma cells and is associated with a poor prognosis and immune rejection of malignant melanoma. Furthermore, *in vitro* and *in vivo*, the study identified that ACSM3 overexpression could reduce the proliferation, invasion and colony formation of malignant melanoma (11). Consistent with the aforementioned report, the present study demonstrated that ACSM3 expression was downregulated in melanoma cells compared with healthy cells. Furthermore, survival analysis using the GEPIA database demonstrated that low levels of ACSM3 were significantly associated with poor overall survival. Therefore, it can be hypothesized that ACSM3 is associated with the clinical malignancy of melanoma.

ACSM3 was therefore considered to be an effective target for the treatment of melanoma and was selected for further study. According to the results of the GEPIA and ChIP assay, KLF10 was positively associated with ACSM3 expression in cutaneous melanoma. KLF10 was demonstrated to bind to and promote the transcription of ACSM3. As KLF10 was demonstrated to be involved in the progression of melanoma, it was hypothesized that KLF10 may target ACSM3 to inhibit the proliferation, migration and invasion of melanoma cells and promote cell apoptosis. Therefore, silencing of ACSM3 was performed. The results demonstrated that silencing ACSM3 reversed the inhibitory effects of KLF10 overexpression on the viability, proliferation, migration and invasion of A375 cells, which indicated that there may be an important interaction between the two molecules.

Furthermore, the mechanism of KLF10 as a tumor suppressor gene of melanoma was preliminarily explored. Akt is considered to be an important component of the cell cycle and in cell survival and apoptosis, and is positively associated with PI3K (27,28). Yang *et al* (29) reported that KLF10 inhibits the PTEN/PI3K/Akt signaling pathway and inhibits the malignant progression of myeloma. Furthermore, Li *et al* (30) demonstrated that LINC00641 inhibits the activation of the PTEN/PI3K/Akt signaling pathway via KLF10 and that activation of this signaling pathway promotes bladder cancer. In the present study, it was demonstrated that KLF10 overexpression in A375 cells decreased the levels of p-PI3K and p-Akt, which indicated that the PI3K/Akt signaling pathway may be negatively regulated by KLF10 expression. These results suggested that the inhibition of A375 cell proliferation, migration and invasion may be dependent on the inactivation of the PI3K/Akt signaling pathway induced by KLF10. Furthermore, PI3K/Akt signaling pathway inactivation induced by KLF10 overexpression was reversed by sh-ACSM3. These results indicated that KLF10 upregulation of ACSM3 may inhibit the malignant progression of A375 cells via the PI3K/Akt signaling pathway. Finally, one limitation of the present study was that only the effect of KLF10 overexpression of KLF10 on melanoma cells *in vivo* was investigated. Further verification experiments involving knockdown of KLF10 would enrich the current research results.

In conclusion, to the best of our knowledge, the present study was the first to elucidate the role of KLF10 in melanoma progression. The results demonstrated that the KLF10/ACSM3/PI3K/Akt axis was associated with melanoma cell proliferation. It was also indicated that KLF10 may inhibit A375 cell proliferation and migration by binding to ACSM3, resulting in the inactivation of the PI3K/Akt signaling pathway. Overall, the present study highlighted a novel mechanism underlying the pathogenesis of melanoma.

Acknowledgements

Not applicable.

Funding

No funding was received.

Availability of data and materials

The datasets used and/or analyzed during the current study are available from the corresponding author on reasonable request.

Authors' contributions

ZZ, YZ and LJ conceptualized and designed the current study. ZZ, YZ, LJ and HZ acquired, analyzed and interpreted the data. LJ and HZ drafted the manuscript and revised it critically for important intellectual content. All authors agreed to be held accountable for the current study in ensuring questions related to the integrity of any part of the work are appropriately investigated and resolved. All authors read and approved the final manuscript. ZZ and HZ confirm the authenticity of all the raw data.

Ethics approval and consent to participate

Not applicable.

Patient consent for publication

Not applicable.

Competing interests

The authors declare that they have no competing interests.

References

1. Raimondi S, Suppa M and Gandini S: Melanoma epidemiology and sun exposure. Acta Derm Venereol 100: adv00136, 2020.
2. Situm M, Buljan M, Kolić M and Vučić M: Melanoma-clinical, dermatoscopical, and histopathological morphological characteristics. Acta Dermatovenerol Croat 22: 1-12, 2014.
3. Davis LE, Shalin SC and Tackett AJ: Current state of melanoma diagnosis and treatment. Cancer Biol Ther 20: 1366-1379, 2019.
4. Soenksen LR, Kassis T, Conover ST, Marti-Fuster B, Birkenfeld JS, Tucker-Schwartz J, Naseem A, Stavert RR, Kim CC, Senna MM, *et al*: Using deep learning for dermatologist-level detection of suspicious pigmented skin lesions from wide-field images. Sci Transl Med 13: eabb3652, 2021.
5. Teramoto Y, Keim U, Gesierich A, Schuler G, Fiedler E, Tüting T, Ulrich C, Wollina U, Hassel JC, Gutzmer R, *et al*: Acral lentiginous melanoma: A skin cancer with unfavourable prognostic features. A study of the German central malignant melanoma registry (CMMR) in 2050 patients. Br J Dermatol 178: 443-451, 2018.
6. Longvert C and Saiag P: Melanoma update. Rev Med Interne 40: 178-183, 2019 (In French).
7. Turner J and Crossley M: Mammalian Kruppel-like transcription factors: More than just a pretty finger. Trends Biochem Sci 24: 236-240, 1999.
8. Chang VH, Chu PY, Peng SL, Mao TL, Shan YS, Hsu CF, Lin CY, Tsai KK, Yu WC and Ch'ang HJ: Kruppel-like factor 10 expression as a prognostic indicator for pancreatic adenocarcinoma. Am J Pathol 181: 423-430, 2012.
9. Zhou M, Chen J, Zhang H, Liu H, Yao H, Wang X, Zhang W, Zhao Y and Yang N: KLF10 inhibits cell growth by regulating PTTG1 in multiple myeloma under the regulation of microRNA-106b-5p. Int J Biol Sci 16: 2063-2071, 2020.
10. Jin W, Chen BB, Li JY, Zhu H, Huang M, Gu SM, Wang QQ, Chen JY, Yu S, Wu J and Shao ZM: TIEG1 inhibits breast cancer invasion and metastasis by inhibition of epidermal growth factor receptor (EGFR) transcription and the EGFR signaling pathway. Mol Cell Biol 32: 50-63, 2012.
11. Zhu Z, Wang D and Shen Y: Loss of ACSM3 confers worsened prognosis and immune exclusion to cutaneous melanoma. J Cancer 11: 6582-6590, 2020.
12. Yan L, He Z, Li W, Liu N and Gao S: The overexpression of Acyl-CoA Medium-Chain Synthetase-3 (ACSM3) suppresses the ovarian cancer progression via the inhibition of integrin β1/AKT signaling pathway. Front Oncol 11: 644840, 2021.
13. Ruan HY, Yang C, Tao XM, He J, Wang T, Wang H, Wang C, Jin GZ, Jin HJ and Qin WX: Downregulation of ACSM3 promotes metastasis and predicts poor prognosis in hepatocellular carcinoma. Am J Cancer Res 7: 543-553, 2017.
14. Kim J, Shin S, Subramaniam M, Bruinsma E, Kim TD, Hawse JR, Spelsberg TC and Janknecht R: Histone demethylase JARID1B/KDM5B is a corepressor of TIEG1/KLF10. Biochem Biophys Res Commun 401: 412-416, 2010.
15. Livak KJ and Schmittgen TD: Analysis of relative gene expression data using real-time quantitative PCR and the 2(-Delta Delta C(T)) Method. Methods 25: 402-408, 2001.
16. Pavri SN, Clune J, Ariyan S and Narayan D: Malignant melanoma: Beyond the basics. Plast Reconstr Surg 138: 330e-340e, 2016.
17. Rastrelli M, Tropea S, Rossi CR and Alaibac M: Melanoma: Epidemiology, risk factors, pathogenesis, diagnosis and classification. In Vivo 28: 1005-1011, 2014.
18. Elder DE, Bastian BC, Cree IA, Massi D and Scolyer RA: The 2018 World health organization classification of cutaneous, mucosal, and uveal melanoma: Detailed analysis of 9 distinct subtypes defined by their evolutionary pathway. Arch Pathol Lab Med 144: 500-522, 2020.
19. Siegel RL, Miller KD and Jemal A: Cancer statistics, 2020. CA Cancer J Clin 70: 7-30, 2020.
20. Namikawa K and Yamazaki N: Targeted therapy and immunotherapy for melanoma in Japan. Curr Treat Options Oncol 20: 7, 2019.
21. Jin W, Di G, Li J, Chen Y, Li W, Wu J, Cheng T, Yao M and Shao Z: TIEG1 induces apoptosis through mitochondrial apoptotic pathway and promotes apoptosis induced by homoharringtonine and velcade. FEBS Lett 581: 3826-3832, 2007.
22. Baroy T, Kresse SH, Skårn M, Stabell M, Castro R, Lauvrak S, Llombart-Bosch A, Myklebost O and Meza-Zepeda LA: Reexpression of LSAMP inhibits tumor growth in a preclinical osteosarcoma model. Mol Cancer 13: 93, 2014.
23. Hsu CF, Sui CL, Wu WC, Wang JJ, Yang DH, Chen YC, Yu WC and Chang HS: Klf10 induces cell apoptosis through modulation of BI-1 expression and Ca2+ homeostasis in estrogen-responding adenocarcinoma cells. Int J Biochem Cell Biol 43: 666-673, 2011.
24. Junkova K, Mirchi LF, Chylíková B, Janků M, Šilhavý J, Hüttl M, Marková I, Miklánková D, Včelák J, Malínská H, *et al*: Hepatic transcriptome profiling reveals lack of Acsm3 expression in polydactylous rats with high-fat diet-induced hypertriglyceridemia and visceral fat accumulation. Nutrients 13: 1462, 2021.
25. De Preter V, Arijs I, Windey K, Vanhove W, Vermeire S, Schuit F, Rutgeerts P and Verbeke K: Impaired butyrate oxidation in ulcerative colitis is due to decreased butyrate uptake and a defect in the oxidation pathway. Inflamm Bowel Dis 18: 1127-1136, 2012.
26. Gopal R, Selvarasu K, Pandian PP and Ganesan K: Integrative transcriptome analysis of liver cancer profiles identifies upstream regulators and clinical significance of ACSM3 gene expression. Cell Oncol (Dordr) 40: 219-233, 2017.
27. Xu F, Na L, Li Y and Chen L: Roles of the PI3K/AKT/mTOR signalling pathways in neurodegenerative diseases and tumours. Cell Biosci 10: 54, 2020.
28. Chen H, Zhou L, Wu X, Li R, Wen J, Sha J and Wen X: The PI3K/AKT pathway in the pathogenesis of prostate cancer. Front Biosci (Landmark Ed) 21: 1084-1091, 2016.
29. Yang N, Chen J, Zhang H, Wang X, Yao H, Peng Y and Zhang W: LncRNA OIP5-AS1 loss-induced microRNA-410 accumulation regulates cell proliferation and apoptosis by targeting KLF10 via activating PTEN/PI3K/AKT pathway in multiple myeloma. Cell Death Dis 8: e2975, 2017.
30. Li Z, Hong S and Liu Z: LncRNA LINC00641 predicts prognosis and inhibits bladder cancer progression through miR-197-3p/KLF10/PTEN/PI3K/AKT cascade. Biochem Biophys Res Commun 503: 1825-1829, 2018.